

# Match and Locate: low-frequency monocular odometry based on deep feature matching

Stepan Konev, Yuriy Biktairov

stevenkonev@gmail.com,  
biktairo@usc.edu

## Abstract

Accurate and robust pose estimation plays a crucial role in many robotic systems. Popular algorithms for pose estimation typically rely on high-fidelity and high-frequency signals from various sensors. Inclusion of these sensors makes the system less affordable and much more complicated. In this work we introduce a novel approach for the robotic odometry which only requires a single camera and, importantly, can produce reliable estimates given even extremely low-frequency signal of around one frame per second. The approach is based on matching image features between the consecutive frames of the video stream using deep feature matching models. The resulting coarse estimate is then adjusted by a convolutional neural network, which is also responsible for estimating the scale of the transition, otherwise irretrievable using only the feature matching information. We evaluate the performance of the approach in the AISG-SLA Visual Localisation Challenge and find that while being computationally efficient and easy to implement our method shows competitive results with only around  $3^\circ$  of orientation estimation error and  $2m$  of translation estimation error taking the third place in the challenge.

## 1 Introduction

Pose estimation is an essential part of many robotics systems. While some systems may afford carrying many sensors and processing complex algorithms that can utilize incoming data, other systems' resources might be very limited however still requiring reliable solutions. These limitations may include low frequency sensor data along with limitation for number of sensors and their broad availability. The proposed method allows to bypass these limitations for efficient and robust camera pose estimation based on low-frequency RGB images.

Our approach is based on using a two-stage model for predicting the relative pose change between the each pair of consecutive time frames. Given the relative poses we then compose them in order to obtain the complete trajectory in the image frame of the first timestamp.

The first stage of the model is a traditional pose estimation technique based on feature matching. It is capable of accurately estimating the relative rotation of the camera provided that there are enough objects present in both images simultaneously.

The second stage is a convolutional neural network predicting the adjustment to the first stage estimate. This model is supposed to correct any systematic inaccuracy of the first stage predictor as well as provide an accurate estimate of the relative translation's magnitude, which the first stage model is not able to do.

## 2 Problem setting challenges

Since the experimental setting we analyze in this work is quite specific we first highlight several important details distinguishing it from the traditional monocular odometry.

Affordable cameras we consider may not have a perfectly stable connection to the computing system processing the signal. Occasionally, the signal might be lost for tens of seconds. When this happens the last image before the interruption and the first image after might not share any identifiable features. In these situations we cannot hope to estimate the relative pose change accurately.

These affordable cameras may also not have a perfectly consistent framerate. Meaning that the distribution of the time intervals between consecutive frames is continuous and might have a considerably heavy tail. This observation motivates us to pay special attention to the timestamps of the frames instead of assuming a regular time grid.

A part of the image might contain a portion of the actual robotic system the camera is mounted on. This portion's image would typically be static and would not provide any relevant information about the relative pose change between the frames. To this extent, we trim any static object present on the image off.

Finally, the lighting conditions may vary a lot between different scenes. The difference might be especially pronounced when images are taken by an affordable camera with no sophisticated post-processing capabilities. The models we use should then, ideally, be robust to the perturbations of this sort.

These observations guide the design of our approach and motivate some of the heuristics we use.

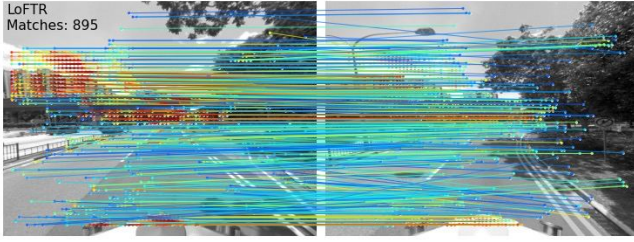


Figure 1: Example of a set of matches between two images.

### 3 Matching-based localization

At the heart of our approach is the classic technique of reconstructing the relative pose between two camera images based on a set of matched points  $M = \{(x_i, y_i)\}$ , where  $x_i \in I_1$  and  $y_i \in I_2$ . Each match  $(x, y)$  indicates that point  $x$  in the first image  $I_1$  and point  $y$  in the second image  $I_2$  both correspond to the same original point in the 3d space. Figure 1 illustrates the idea by connecting the matched points with a colored line. Given an accurate enough set of at least 8 matches we can reconstruct the relative pose between the cameras up to a scale factor. The scale factor cannot be determined based solely on camera images: intuitively, images only contain the information regarding the directions of rays coming to the camera, but these directions stay the same when we scale the world up or down.

#### 3.1 Deep feature matching models

Traditionally, so-called sparse feature matching is used for this kind application. The most prominent example of such application would be the monocular visual SLAM, frequently used as a localisation solution for drones and in-door robots. Sparsity implies that only select points from each image are attempted to be matched against each other. The selection criterion is usually based on a kind of edge detection algorithm and the matching relies on comparing a set of features extracted from around the candidate points.

These techniques work quite good for the high framerate (or, alternatively, slow motion) situations, where the relative pose between the consecutive frames is not far from the identity pose. This is not the case, however, in our setting where the typical time interval between the frames is around  $1s$  and the system’s speed is on the scale of  $10m/s$ . Sometimes the relative pose comprises such a big rotation that the consecutive images do not have any semantic intersection. For this reason we use dense feature matching instead.

Dense feature matching algorithms do not rely on finding distinct boundaries between objects and produce higher number of matches along with the confidence scores for each match. Recently, a number of deep-learning-based models for dense feature matching were published. According to the evaluation results these are capable of producing decent matches even for drastically different camera poses. We experimented with LoFTR[Sun *et al.*, 2021], DKM [Edstedt *et al.*, 2022] and CoTracker[Karaev *et al.*, 2023] feature matching models and found the former to be better suited for our task.

#### 3.2 Pose reconstruction

The go-to approach to the matching-based pose reconstruction is the RANSAC algorithm[Fischler and Bolles, 1981] capable of handling a large number of erroneous matches, or a more recent development of the algorithm – GC-RANSAC[Barath and Matas, 2018].

During our evaluation we found that GC-RANSAC does not provide noticeable improvement over the conventional RANSACK, so we used the latter for our main model. Another set of evaluations shows that the optimal values of parameters for our case are

$$\begin{aligned} prob &= 0.99999, \\ threshold &= 0.9. \end{aligned}$$

#### 3.3 Coarse translation estimation

Since the scale of the relative pose cannot be determined by the images alone, we use the following simple heuristic for our base model: we assume that the absolute value of the translation is the same for every pair of consecutive frames in the trajectory. This simplification is inaccurate since there are both stationary sections and long temporal discontinuities present in the train trajectories. It is, however, a decent base for the refinement model to build upon.

We choose this constant translation’s magnitude to be  $10m$  based on running the approach on the training set in our experimental evaluation.

#### 3.4 Constant rotation heuristic

Another important heuristic we use covers the pairs of frames where no meaningful semantic intersection is present between the images. We use the number of matches with high enough confidence scores as an indicator that such a situation is encountered.

Similarly to the translation heuristic, here we assume a constant rotation. We notice that the movement of the camera is generally flat, so we assume a rotation around the vertical axis which almost coincides with  $x$  axis of the image frame. As to the value of this rotation – we choose  $\pi$  as in many cases such a situation can be attributed to the system making a u-turn or a similar maneuver.

### 4 CNN refinement model

Given a matching-based backbone model, we train a convolutional neural network to predict adjustments to the estimate provided by the backbone. Introducing this second stage to the pipeline can potentially lead to the following improvements:

- CNN can provide sensible non-constant estimates of the translation;
- CNN can adjust the prior rotation based on the actual statistics of the dataset;
- CNN can compensate for any systematic bias in the matching-based model.

## 4.1 Additional features

In order to facilitate the training of the refinement model we preprocess the dataset by adding three feature maps:

1. the monocular depth estimate of the first frame extracted by MiDaS[Ranftl *et al.*, 2020];
2. the monocular depth estimate of the second frame extracted by MiDaS;
3. the optical flow estimate extracted by RAFT[Teed and Deng, 2020];
4. time interval encoding;

These feature maps are only extracted once. We do not train the corresponding models and do not extract the features again after augmenting the RGB images during training.

## 4.2 Architecture

We experimented with several pre-trained convolutional vision models from timm[Wightman, 2019] including versions of EfficientNet[Tan and Le, 2019] and ResNet[He *et al.*, 2016],

## 4.3 Pose representation

For the training purposes we represent the relative pose as a pair of  $3d$  translation vector and  $4d$  unit quaternion corresponding to the rotation. We model the predicted translation as the sum of the matching-based estimate and the output of the final linear layer of the CNN

$$t = t_{base} + t_{CNN}.$$

We model the predicted rotation in a similar way, normalizing the result to preserve the unitary length of the quaternion

$$q = \frac{q_{base} + q_{CNN}}{|q_{base} + q_{CNN}|}.$$

In some evaluations we also eliminate the ambiguity of representing a rotation with a quaternion by enforcing  $w > 0$ . We do it by transforming the real part of the quaternion prior to normalization

$$w = \exp(w_{prelim}).$$

While it does eliminate the ambiguity and should, therefore, enhance the generalization, it also makes representation the rotations of magnitude  $\sim \pi$  discontinuous. It makes the performance of such standardisation highly dependent on the structure of the dataset. We couldn't make a decisive conclusion in this regard.

The loss function we use for training directly mimics the metrics used for the evaluation

$$L_r = 2 \arccos(|q \cdot q_{GT}|),$$

$$L_t = |t - t_{GT}|_2,$$

where we linearly extrapolate  $\arccos$  in the interval  $[1 - \varepsilon, 1]$  in order to avoid infinite gradients.

Table 1: Experimental evaluation.

Model	$R_r^{pub.}$	$R_r^{priv.}$	$R_t^{priv.}, m$
2 <sup>nd</sup> stage only	0.041	0.094	12.0
2 <sup>nd</sup> stage only + aug.	0.039	0.072	11.7
2 <sup>nd</sup> stage ensemble	0.043	0.069	10.8
2 <sup>nd</sup> stage ensemble + aug.	0.041	0.064	11.0
both stages	<b>0.032</b>	<b>0.046</b>	<b>2.0</b>

## 4.4 Augmentations

As the training dataset is quite limited we use a vast range of augmentations in order to facilitate the generalization of the CNN model.

We apply a big suite of standard visual augmentations supported by Albumentations[Buslaev *et al.*, 2020] to the model so it can more easily generalize to new lighting conditions.

We use the approximate planarity of motion again and introduce the vertical reflection of the images as an augmentation. This transformation does not really preserve the distribution over the images since the left-hand-side roads become right-hand-side, but these high-level changes should not affect the basic localisation task too much. Reflection of the images should also be accompanied with the corresponding amendments to the optical flow map and the target relative pose.

Finally, we augment the dataset by applying a perspective transformation corresponding to small additional rotation of the camera to the second image. We then crop the image to hide the border, where we might not have the image values after the transformation. This transformation also requires adjusting the target relative pose and optical flow map.

## 5 Inference time

Running on a machine with an nvidia rx 3090 GPU our approach takes around  $\sim 1s$  to process a single pair of consecutive images. With the typical framerate of the trajectories in the dataset also being close to  $1s$  we are confident that with a couple optimizations the approach may be robustly run in real time.

## 6 Evaluation

We evaluate our approach in the AISG-SLA Visual Localisation Challenge. The results of this evaluation are displayed in table 1.

The upper four models do not use matching-based coarse estimates as a baseline. They only contain stage 2 of our approach: a CNN predicting the  $6d$  pose. The results indicate that applying augmentations we designed for the training is beneficial for both a single CNN model and an ensemble of models. The results also suggest that an ensemble of CNNs generalizes better to the private testing dataset, which is a known effect of ensembling.

Finally, the last entry in table 1 shows the performance of our complete model with both stages enabled. We can clearly see that the first matching-based stage of the approach is indeed very important and improves the results significantly.

## References

- [Barath and Matas, 2018] Daniel Barath and Jiří Matas. Graph-cut ransac. In *Proceedings of the IEEE conference on computer vision and pattern recognition*, pages 6733–6741, 2018.
- [Buslaev *et al.*, 2020] Alexander Buslaev, Vladimir I Iglovikov, Eugene Khvedchenya, Alex Parinov, Mikhail Druzhinin, and Alexandr A Kalinin. Albumentations: fast and flexible image augmentations. *Information*, 11(2):125, 2020.
- [Edstedt *et al.*, 2022] Johan Edstedt, Ioannis Athanasiadis, Mårten Wadenbäck, and Michael Felsberg. Dkm: Dense kernelized feature matching for geometry estimation, 2022.
- [Fischler and Bolles, 1981] Martin A Fischler and Robert C Bolles. Random sample consensus: a paradigm for model fitting with applications to image analysis and automated cartography. *Communications of the ACM*, 24(6):381–395, 1981.
- [He *et al.*, 2016] Kaiming He, Xiangyu Zhang, Shaoqing Ren, and Jian Sun. Deep residual learning for image recognition. In *Proceedings of the IEEE conference on computer vision and pattern recognition*, pages 770–778, 2016.
- [Karaev *et al.*, 2023] Nikita Karaev, Ignacio Rocco, Benjamin Graham, Natalia Neverova, Andrea Vedaldi, and Christian Rupprecht. Cotracker: It is better to track together. *arXiv preprint arXiv:2307.07635*, 2023.
- [Ranftl *et al.*, 2020] René Ranftl, Katrin Lasinger, David Hafner, Konrad Schindler, and Vladlen Koltun. Towards robust monocular depth estimation: Mixing datasets for zero-shot cross-dataset transfer. *IEEE transactions on pattern analysis and machine intelligence*, 44(3):1623–1637, 2020.
- [Sun *et al.*, 2021] Jiaming Sun, Zehong Shen, Yuang Wang, Hujun Bao, and Xiaowei Zhou. Loftr: Detector-free local feature matching with transformers. In *Proceedings of the IEEE/CVF conference on computer vision and pattern recognition*, pages 8922–8931, 2021.
- [Tan and Le, 2019] Mingxing Tan and Quoc Le. Efficientnet: Rethinking model scaling for convolutional neural networks. In *International conference on machine learning*, pages 6105–6114. PMLR, 2019.
- [Teed and Deng, 2020] Zachary Teed and Jia Deng. Raft: Recurrent all-pairs field transforms for optical flow. In *Computer Vision—ECCV 2020: 16th European Conference, Glasgow, UK, August 23–28, 2020, Proceedings, Part II 16*, pages 402–419. Springer, 2020.
- [Wightman, 2019] Ross Wightman. Pytorch image models. <https://github.com/rwightman/pytorch-image-models>, 2019.